Acetylene Chemisorption on Sn/Pt(100) Alloys†

ARTICLE *in* THE JOURNAL OF PHYSICAL CHEMISTRY B · APRIL 2001

Impact Factor: 3.3 · DOI: 10.1021/jp003445i

3 AUTHORS, INCLUDING:

Najat A Saliba
American University of Beirut
72 PUBLICATIONS **1,654** CITATIONS
SEE PROFILE

Bruce Koel
Princeton University
296 PUBLICATIONS **9,082** CITATIONS
SEE PROFILE

Acetylene Chemisorption on Sn/Pt(100) Alloys†

Chameli Panja, Najat A. Saliba, and Bruce E. Koel*

University of Southern California, Department of Chemistry, Los Angeles, California 90089-0482

Received: September 23, 2000; In Final Form: March 5, 2001

Adsorption and reaction of acetylene on a hexagonally reconstructed (5 × 20)-Pt(100) surface and two ordered Sn/Pt(100) alloy surfaces were investigated using temperature programmed desorption spectrometry (TPD), Auger electron spectroscopy (AES), low energy electron diffraction (LEED) and X-ray photoelectron spectroscopy (XPS). Vapor deposition of Sn onto a Pt(100) single-crystal substrate was used to form two Pt−Sn alloys, the c(2 × 2) and (3√2×√2)R45° Sn/Pt(100) structures with $\theta_{Sn} = 0.5$ and 0.67 ML, respectively, depending on the initial Sn concentration and annealing temperature. Acetylene nearly completely decomposed during TPD on Pt(100) in the absence of Sn, forming hydrogen, which then desorbs as H_2, and surface carbon. This decomposition, associated with irreversible dissociative adsorption, was strongly suppressed on the two Pt−Sn alloy surfaces, and a large acetylene desorption peak in TPD was observed. Additionally, 15% of the adsorbed acetylene monolayer was converted to gaseous benzene during TPD on the (3√2×√2)-R45° Sn/Pt(100) alloy. No such benzene desorption occurred from the c(2 × 2) alloy. Alloyed Sn in the c(2 × 2) alloy decreased the initial sticking coefficient of acetylene on Pt(100) at 100 K by ∼40%, but additional Sn in the other alloy had no additional effect. The saturation coverage of C_2D_2 in the chemisorbed monolayer at 100 K decreased from that on Pt(100) by 35% on the c(2 × 2) alloy and 50% on the (3√2×√2)-R45° Sn/Pt(100) alloy. However, the c(2 × 2)-Sn adlayer eliminates acetylene chemisorption, illustrating that the effectiveness of Sn to "block" sites depends crucially on its location as an adatom or alloyed atom on Pt surfaces. The acetylene chemisorption bond energy, estimated by the acetylene desorption activation energy measured in TPD, also decreased (45−65%) as the alloyed Sn concentration increased. Multiple TPD peaks for C_2D_2 desorption from both the c(2 × 2) and the (3√2×√2)R45°Sn/Pt(100) alloy surfaces indicate either several energetically distinguishable adsorption sites for acetylene or the rate-limiting influence of more complex surface reactions on these surfaces.

1. Introduction

Acetylene (C_2H_2) chemisorption and reaction on Pt and other transition-metal surfaces has been studied many times, mainly to probe surface reactions related to heterogeneous catalysis. Pt(111) and Pt(100) surfaces are known to be highly reactive toward acetylene decomposition, and the formation of hydrogen and adsorbed carbon on the surface is the only reaction pathway observed in UHV studies.[1−4] Such a high reactivity, which leads to nonspecific carbon build-up, is not desired in most industrial reactions, so commercial hydrocarbon conversion catalysts often utilize bimetallic Pt-based catalysts containing a second metal component in order to modify (reduce) the reactivity of Pt.[5,6] Surface science studies of Pt−Sn alloys have also shown consistent results indicating that hydrocarbon dehydrogenation rates on Pt−Sn alloys were much slower than on clean Pt.[7−9]

As a highly reactive molecule with a C:H stoichiometry of unity, acetylene can serve as a prototype for reactions of "coke precursors." Also, C_2H_2 can be used to probe C−C bond coupling reactions under UHV conditions. Cyclotrimerization of C_2H_2 to form a benzene desorption peak in TPD is a rather unique reaction that occurs only on Pd(111)[10−13] and Cu(110)[14,15] pure-metal surfaces. Lambert and co-workers[10−12] elucidated that the mechanism for this reaction first involves dimerization to form a C_4H_4 metallopentacyclic intermediate, which then forms benzene with a third C_2H_2 molecule in an associative mechanism without cleavage of any C−C or C−H bonds.[10−12] On Ni(111), there is evidence of benzene formation on the surface at high C_2H_2 coverages[16] (or from CH_3 dosing[17]), but it apparently decomposes during heating to desorb H_2 and leave carbon on the surface. The clean Pt(111) surface does not desorb benzene from this reaction.[1−3]

Acetylene cyclotrimerization on Pd single-crystal surfaces is sensitive to both the atomic geometry and the electronic structure of the metal surface. For example, benzene formation is more efficient on Pd(111) than on Pd(100) and Pd(110) surfaces.[18] Also, the presence of sulfur enhanced the degree of benzene formation on Pd surfaces.[18] More recently, this reaction was found to be effectively carried out on reduced TiO_2(001)[19] and several bimetallic alloys.[20−23] We are particularly interested in these latter results because bimetallic alloys provide the possibility of investigating the nature of the surface metal atom ensemble and site requirements for such cyclization activity. Benzene desorption from cyclotrimerization of acetylene has been observed on Sn/Pt(111),[20] Au/Pd(111),[21] and Pd/Au(111)[22,23] alloy surfaces.

We have previously studied C_2H_2 adsorption and reaction on two ordered, Pt−Sn surface alloys formed on Pt(111). These alloys have (2 × 2) and (√3×√3)R30° unit cells, with $\theta_{Sn} =$ 0.25 and 0.33 ML in the outermost layer, respectively.[24,25] Decomposition of acetylene was strongly suppressed by alloying Sn in the surface layer of Pt(111), and benzene desorption was observed on both alloys.[20] On the (√3×√3)R30° alloy, which desorbed more benzene than the (2 × 2) alloy, 33% of the

† Part of the special issue "John T. Yates, Jr. Festschrift".

* To whom correspondence should be addressed.

10.1021/jp003445i CCC: $20.00
Published on Web 04/14/2001

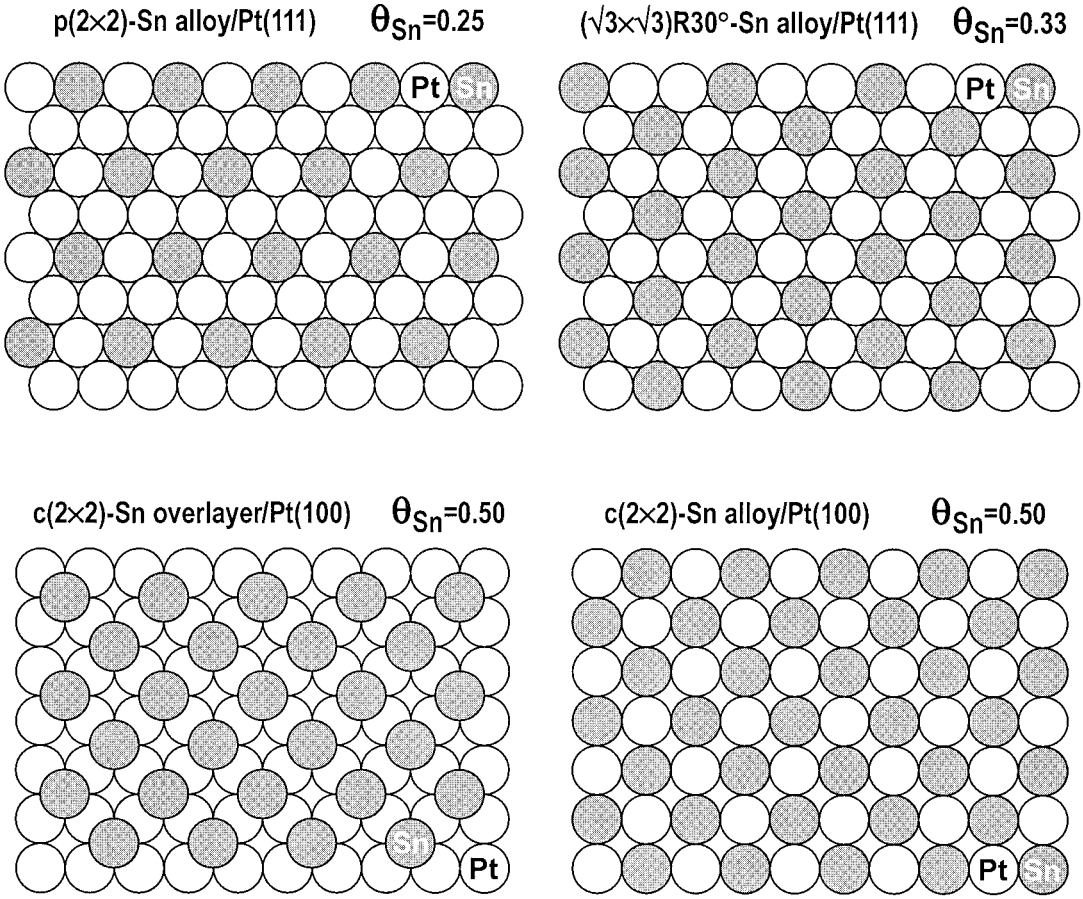

Figure 1. Schematic top view of the structures of the (2 × 2) and ($\sqrt{3}\times\sqrt{3}$)R30° Sn/Pt(111) surface alloys (top) and the c(2 × 2)-Sn overlayer on Pt(100) and c(2 × 2)Sn/Pt(100) alloy (bottom).

adsorbed acetylene monolayer decomposed to form carbon and hydrogen on the surface and 10% of the adsorbed acetylene cyclotrimerized to form benzene (under the given TPD conditions). On Pd(111), a relatively weak interaction of C_2H_2 preserves the alkyne bond character, in contrast to the strong rehybridization on Pt, Rh, and Ir, and this contributes to benzene formation.[10−13] Similarly, Sn in the two Pt−Sn alloys studied weakens the acetylene−surface interaction and decreases the activity for decomposition, thus facilitating benzene formation.[20]

We report herein on C_2D_2 adsorption on a hexagonally reconstructed (5 × 20)-Pt(100) surface, referred to as the "hex" phase,[26] and two additional, ordered Pt−Sn alloys that can be formed by heating Sn films deposited on a Pt(100) single crystal. These alloys have c(2 × 2) and ($3\sqrt{2}\times\sqrt{2}$)R45° unit cells, with $\theta_{Sn} = 0.5$ and 0.67 ML, respectively, in the topmost layer.[27,28] (Herein we refer to 1 ML = 1.303×10^{15} atoms cm^{-2}, which is the unreconstructed Pt(100) surface atom density.) Both of these alloys have higher surface Sn concentrations than the two surface alloys on Pt(111) that were previously studied. On the c(2 × 2) Sn/Pt(100) alloy, each Pt atom has only Sn atom nearest neighbors, forming a "checker-board" pattern of isolated Pt atoms surrounded by Sn atoms. This alloy can be used to probe the reactivity of single Pt-atom reactive ensembles. Low energy alkali ion scattering spectroscopy (ALISS) results suggest that the ($3\sqrt{2}\times\sqrt{2}$)R45° alloy has nearly the same geometric structure as the c(2 × 2) alloy and is composed of small c(2 × 2)-alloy domains with the same buckling distance within the domains.[28] However, the structure of this surface has not been fully determined.

In this paper, we probe the influence of alloyed Sn on Pt for (i) suppressing the decomposition of acetylene and thereby reducing carbonaceous accumulation, and (ii) forming gaseous benzene by acetylene cyclotrimerization. XPS measurements were performed to estimate the C_2H_2 coverage on hex-Pt(100) and the two Pt−Sn alloys. We also investigated the chemistry of a c(2 × 2)-Sn/Pt(100) adlayer for comparison.

2. Experimental Methods

All of the experiments were performed in a two-level, stainless steel, ultrahigh vacuum (UHV) chamber with a base pressure of 8×10^{-11} Torr, which has been described elsewhere.[29] It was equipped with a low energy electron diffraction (LEED) optics, double-pass cylindrical mirror analyzer (CMA) for AES and XPS, ion-sputtering gun, UTI 100C quadrupole mass spectrometer (QMS) for TPD, dual anode X-ray source for XPS, and facilities for directed-beam gas dosing and metal evaporation.

The Pt(100) crystal was cleaned by repeated cycles of Ar^+ ion sputtering at 300 K and oxygen treatments with $P_{O_2} = 5 \times 10^{-7}$ Torr while the Pt crystal was held at 1200 K. The cleanliness of the crystal was checked by AES, and LEED showed the expected reconstruction, i.e., the (5 × 20)-Pt(100) pattern.[26] The manipulator allowed for the Pt crystal to be resistively heated to 1240 K and cooled to 95 K by contact with a liquid nitrogen reservoir. The temperature was measured by a chromel−alumel thermocouple that was spot-welded to the side of the crystal.

Acetylene (C_2D_2) (Cambridge Isotope Laboratories, 99.96%) was used without further purification. Gas exposures reported herein have been corrected for an ionization gauge sensitivity factor (1.9) and also a directed beam-doser enhancement factor of 60.[30]

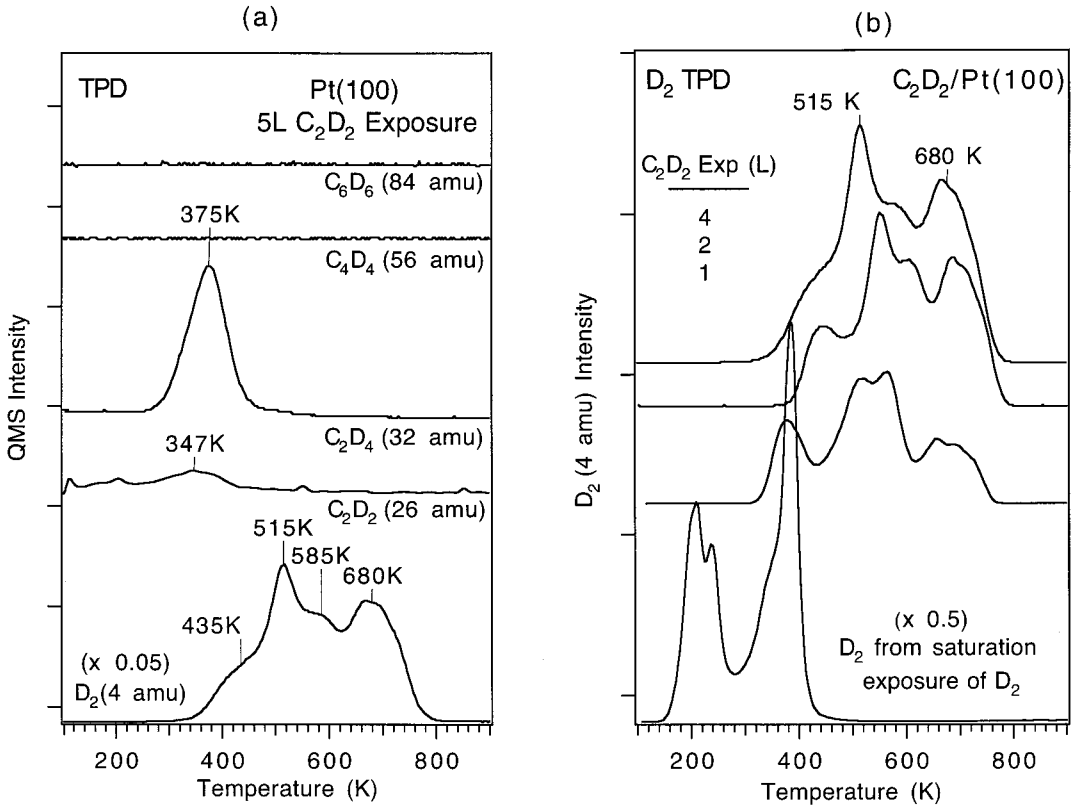

Figure 2. (a) TPD spectra of desorbed products from the decomposition of a saturation monolayer of acetylene on hex-Pt(100). (b) D_2 TPD spectra after C_2D_2 exposures on a hex-Pt(100) surface at 100 K.

All of the TPD experiments were done by using a heating rate of 4 K/s. XPS was carried out by using 300 W Mg Kα radiation ($h\nu = 1253.6$ eV) with the CMA operated at a pass energy of 50 eV ($\Delta E = 0.8$ eV). All binding energies (BE) reported are referenced to the Fermi energy. The Pt($4f_{7/2}$) peak was defined to be 70.90 eV BE.

The c(2 × 2) and ($3\sqrt{2}\times\sqrt{2}$)R45° Sn/Pt(100) alloy surfaces were prepared by evaporating a thin Sn film onto a clean hex-Pt(100) surface at 300 K and then annealing the sample to 750 or 900 K, respectively, as described by Paffett et al.[27] The observed c(2 × 2) LEED pattern following Sn deposition on Pt(100) could be due to two different surface structures.[27,28] An overlayer of Sn adatoms is formed over a relatively wide range of temperatures below 750 K. This adlayer is ordered after heating to 500−750 K. Formation of the c(2 × 2) alloy occurs over a narrow range of 750−800 K, depending on the initial Sn concentration. This alloy comprises 0.5 ML of Sn incorporated into the Pt(100) surface plane to form a "checker board" pattern. Each Pt atom is isolated from nearest neighbor Pt-atom contacts, i.e., surrounded by all Sn-atom neighbors, and vice versa.[27] The alloy surface is quite flat, with Sn atoms buckled outward by ~0.20 Å above the surface Pt-atom plane.[28] A more thermally stable alloy with a ($3\sqrt{2}\times\sqrt{2}$)R45° LEED pattern and $\theta_{Sn} = 0.67$ ML is formed at higher annealing temperatures between 800 and 1050 K. This LEED pattern may be the result of a periodic surface reconstruction with Sn atoms occupying the domain boundaries.[27] ALISS experiments suggest that the ($3\sqrt{2}\times\sqrt{2}$)R45° alloy has nearly the same local geometric structure as the c(2 × 2) alloy and is at least partially composed of small c(2 × 2) alloy domains with the same buckling distance within the domains.[28] However, the structure of this surface is still undetermined. Recent STM images of a somewhat related (100) surface of a bulk Pt_3Sn alloy, after sputtering and annealing to 600 K, show pyramidal features consisting of (102) facets.[31] Flat portions between and on top of the pyramids formed by the facets are mainly composed of triple rows that are probably Pt. A c(2 × 2) LEED pattern with streaky facet spots was observed after heating to 600 K, and an improved c(2 × 2) LEED pattern with no facet spots occurred after annealing to 1000 K.[31] STM studies in our lab are planned to further probe the structure of the ($3\sqrt{2}\times\sqrt{2}$)R45° Sn/Pt(100) alloy and the relationship that its structure has to that of other surface alloys and bulk alloy surfaces. Real space models of the (2 × 2) and ($\sqrt{3}\times\sqrt{3}$)*R*30° Sn/Pt(111) alloys, the c(2 × 2)-Sn overlayer on Pt(100), and the c(2 × 2) Sn/Pt(100) alloy are shown in Figure 1.

For brevity, we will refer to the c(2 × 2)Sn/Pt(100) and the ($3\sqrt{2}\times\sqrt{2}$)R45° Sn/Pt(100) alloys simply as the c(2 × 2) and $3\sqrt{2}$ alloys, respectively, throughout this paper.

3. Results

3.1. TPD. Thermal desorption spectra following adsorption of a chemisorbed monolayer of d_2-acetylene (C_2D_2) on the clean hex-Pt(100) surface is shown in Figure 2a. At low initial C_2D_2 coverages, completely irreversible adsorption of C_2D_2 occurred. d_2−Acetylene decomposed during TPD to liberate only $D_{2(g)}$ and form a carbon adlayer. In addition to D_2, a small amount of C_2D_4 and C_2D_2 desorbed at higher coverages. No desorption of other hydrocarbons such as C_2D_6 (ethane), C_3D_8 (propane), C_3D_6 (propene), C_4D_x species, or C_6D_6 (benzene) was detected. Hence, C_2D_2 adsorption is essentially irreversible on the Pt-(100) surface, with no dimerization or trimerization products formed during TPD. This is consistent with the results of a previous study.[4]

Figure 2b shows D_2 evolution from the Pt(100) surface during TPD after increasing C_2D_2 exposures on hex-Pt(100) at 100 K. The bottom curve provides the D_2 TPD trace after a saturation

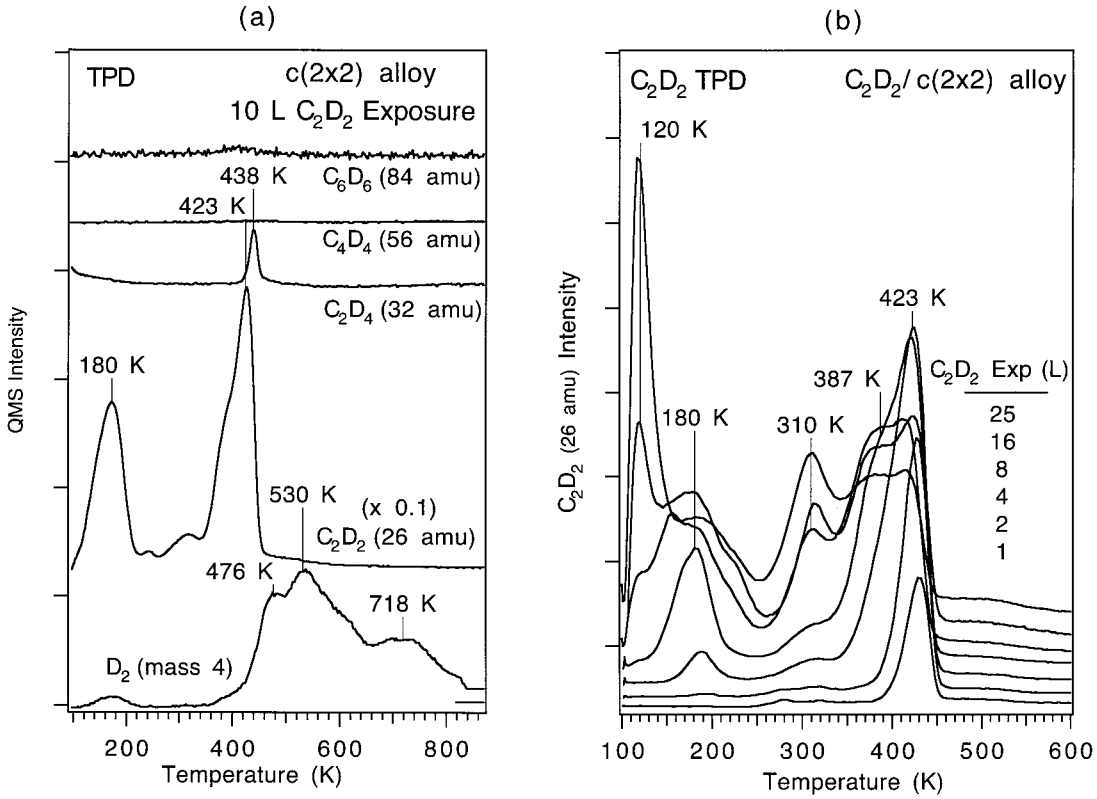

Figure 3. (a) TPD spectra obtained after a saturation exposure of acetylene on the c(2 × 2) Sn/Pt(100) alloy at 100 K. (b) C_2D_2 TPD spectra obtained following several acetylene exposures on the c(2 × 2) Sn/Pt(100) alloy at 100 K.

exposure of D_2 on the hex-Pt(100) surface at 100 K to give θ_D = 1.20 ML.[32] By comparing this curve with those from C_2D_2 decomposition, we conclude that the lowest temperature D_2 TPD peak at 378 K could be D_2 desorption rate limited, but all of the other, higher temperature D_2 peaks are clearly rate limited by reactions forming $D_{(a)}$. D_2 desorption shows that at least partial dehydrogenation occurs on Pt(100) at or below 378 K for low initial C_2D_2 coverages. The three high-temperature peaks for D_2 evolution are very similar to those from C_2D_2 on Pt(111),[1−3] so sequential dehydrogenation reactions of acetylene and its decomposition products at higher temperatures may be similar on these two surfaces. Acetylene adsorbs molecularly on Pt(111) below 330 K in a $\mu_3-\eta^2$ configuration, disproportionates to form ethylidyne (CCH_3) and other species (possibly C_2H) between 330 and 400 K, and then undergoes further dehydrogenation to form surface carbon and $H_{2(g)}$.[1−3] Ethylidyne hydrogenation on Pt(111) forms a small amount of $C_2D_{4(g)}$ during TPD, and ethylidyne decomposition causes a characteristic D_2 TPD peak at 435 K.[1−3] The peak near 435 K in Figure 2b may also arise from decomposition of ethylidyne that was formed as a metastable intermediate on Pt(100), but mechanistic information about C_2D_2 decomposition on the Pt(100) surface awaits additional studies.

Products desorbed during TPD after C_2D_2 exposures to form a monolayer on the c(2 × 2) alloy at 100 K are shown in Figure 3a. We monitored the 26-amu signal from a cracking fragment of C_2D_2 in order to exclude contributions from background CO adsorption when evaluating amounts of C_2D_2 adsorption and desorption. The principal desorbed species were C_2D_2 (from reversible adsorption) and D_2. The amount of D_2 desorption corresponded to θ_D = 0.15 ML, as determined by comparison to the D_2 TPD peak area following D_2 exposures on hex-Pt(100) at 100 K. This amount is consistent with the small amount of adsorbed carbon that was found in AES following TPD, and corresponds to $\theta^{dec}_{C_2D_2}$ = 0.022 ML or 7% of the amount of adsorbed C_2D_2 (as shown later). We believe that this is an accurate measure of the reactivity of this surface, but it is difficult to exclude the possibility that defect sites lead to this small amount of C_2D_2 decomposition. We searched for the desorption of other hydrocarbon products, but, except for a small amount of C_2D_4 after large exposures, no other C_2, C_4, or C_6 products were found.

Figure 3b shows C_2D_2 TPD curves after increasing exposures of C_2D_2 on the c(2 × 2) alloy at 100 K. A C_2D_2 peak occurs at 430 K even, at low coverages, and this peak shifts down slightly to 423 K at saturation coverage in the chemisorbed layer. After high exposures, peaks appear at 387 and 310 K, whereas the peak at 423 K decreases slightly in size. Desorption from a weakly bonded state also occurs in a peak at 180 K. We believe that this latter peak is due to a species in the chemisorbed monolayer that is π-bonded to the surface rather than due to acetylene adsorbed in the second layer, i.e., first physisorbed layer. We reached this conclusion because the coverage associated with this peak is much less than that of the chemisorbed layer. C_2H_2 multilayers could be formed and cause an apparent peak at 120 K, as reported on Cu(110).[15] But we assign the peak at 120 K to another physisorbed state, possibly on Sn sites, because its intensity does not increase linearly with C_2D_2 exposures.

TPD spectra from the C_2D_2 chemisorbed monolayer on the $3\sqrt{2}$ alloy are shown in Figure 4a. Acetylene was mostly reversibly adsorbed. Again, by using the D_2 TPD peak area, we estimate that $\theta^{dec}_{C_2D_2}$ = 0.012 ML, or ∼5% of the adsorbed acetylene monolayer (as shown later) decomposed during TPD. Interestingly, benzene desorption was observed from this surface following the cyclotrimerization of acetylene.

Figure 4b shows C_2D_2 TPD spectra after increasing acetylene

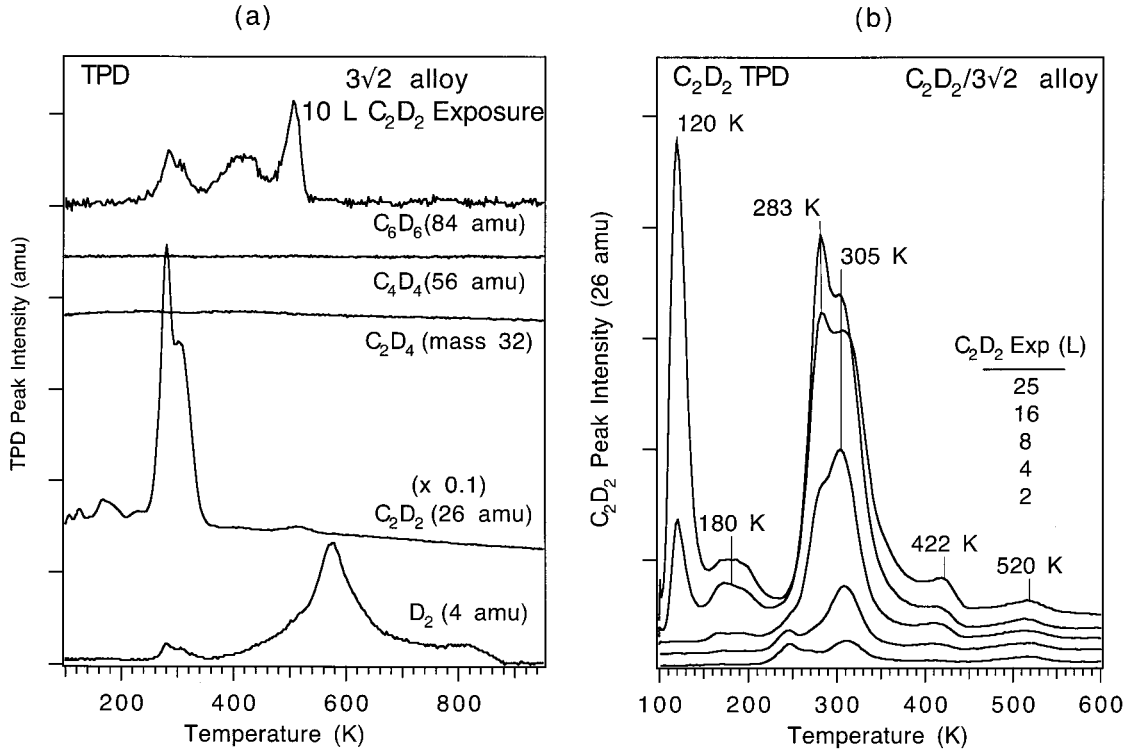

Figure 4. Desorption of products from reactions of a monolayer of acetylene on the $(3\sqrt{2}\times\sqrt{2})$R45° Sn/Pt(100) alloy during TPD. (b) TPD spectra of acetylene after C_2D_2 exposures on the $(3\sqrt{2}\times\sqrt{2})$R45° Sn/Pt(100) alloy at 100 K.

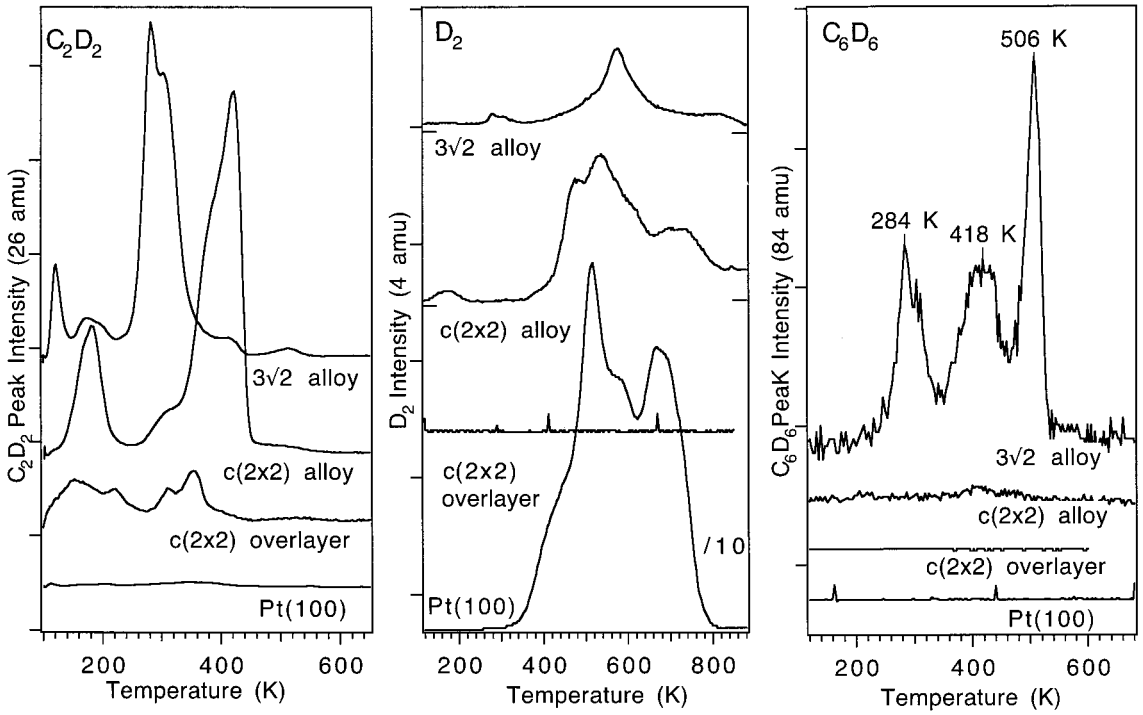

Figure 5. Comparison of C_2D_2, D_2, and C_6D_6 TPD spectra obtained from acetylene monolayers on different surfaces at 100 K.

exposures on the $3\sqrt{2}$ alloy at 100 K. Initially, a peak grows at 305 K and then a second peak grows larger at 283 K. Two small, high-temperature peaks were also observed at 422 and 520 K. As on the c(2 × 2) alloy, peaks at 180 and 120 K were observed and are assigned to two weakly adsorbed, π-bonded C_2D_2 species.

In Figure 5, we compare C_2D_2, D_2, and C_6D_6 TPD spectra following the adsorption and reaction of monolayer coverages of acetylene on several surfaces at 100 K. C_2D_2 is irreversibly adsorbed on the hex-Pt(100) surface, liberating only D_2 in TPD. Sn adatoms in an ordered c(2 × 2) Sn overlayer ($\theta_{Sn} = 0.5$ ML) on the Pt(100) surface allow only a very small amount of chemisorption and completely suppress acetylene decomposition and reaction. (The c(2 × 2)-Sn overlayer was prepared[27,28] by annealing a thin layer of Sn (>0.5 ML) on the hex-Pt(100) to 500 K.) On the c(2 × 2) alloy, also with $\theta_{Sn} = 0.5$ ML, decomposition was strongly reduced during TPD, but the alloy surface retained a large chemisorption capacity. *These spectra*

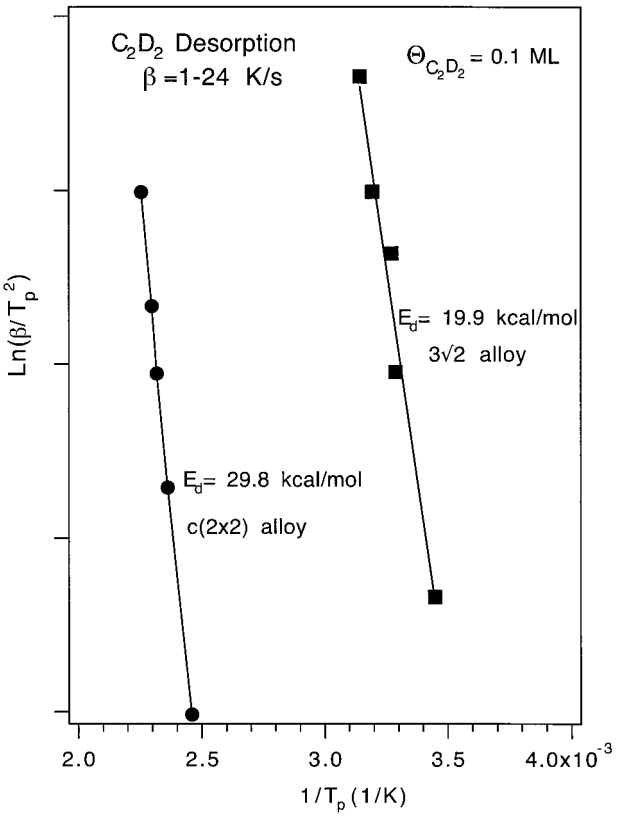

Figure 6. Plots of $\ln(\beta/T_p^2)$ versus $1/T_p$ for thermal desorption of acetylene from the most strongly adsorbed, reversibly bound state on the two Sn/Pt(100) alloys. Heating rates β of 1−24 K/s were used.

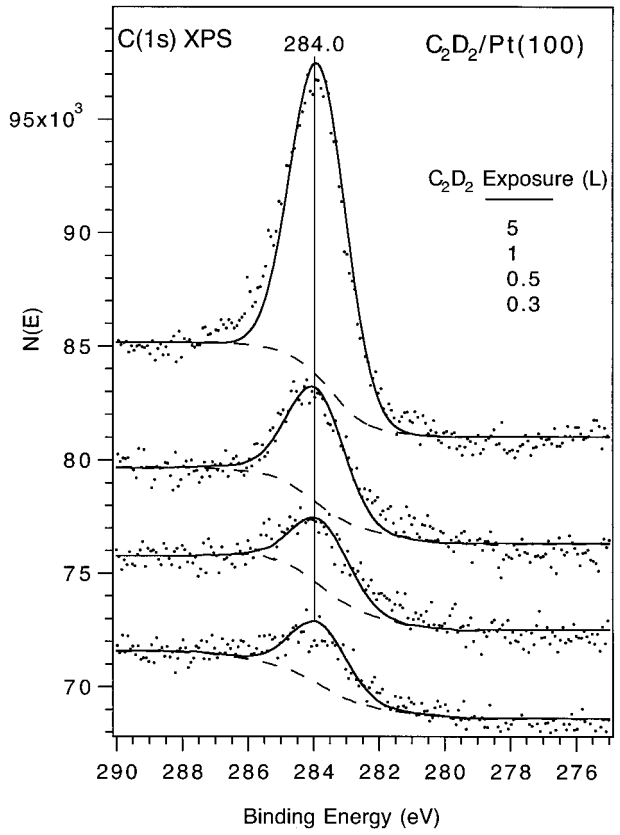

Figure 7. C(1s) XPS spectra taken after acetylene exposures on clean hex-Pt(100) at 100 K.

illustrate an important difference in the effectiveness of Sn to "block" sites depending on its location as an adatom or alloyed atom on Pt surfaces. The most strongly chemisorbed C_2D_2 molecules on the c(2 × 2) alloy desorbed at 423 K, and no benzene desorption was observed. On the $3\sqrt{2}$ alloy, with θ_{Sn} = 0.67 ML, the C_2D_2 adsorption energy is decreased further, as indicated by a shift of the acetylene desorption peak to lower temperatures, and cyclotrimerization reactions form benzene which desorbs from the surface.

To determine the C_2D_2 desorption activation energy (E_d) on the two alloy surfaces, we measured C_2D_2 desorption kinetics and the desorption peak temperature (T_p) using heating rates (β) of 1−24 K/s. We considered only the highest temperature desorption peak at about 10% of the monolayer coverage in order to minimize lateral interactions. Plots of $\ln(\beta/T_p)$ versus $1/T_p$ associated with these measurements are shown in Figure 6. Such plots should yield a straight line with slope = $-E_d/R$, where R is the gas constant, which is independent of the value of the preexponential factor.[33] Values for E_d of 29.8 and 19.9 kcal/mol were determined by this method for the c(2 × 2) and $3\sqrt{2}$ alloy surfaces, respectively. We note that these values are not too different from those of 27 and 19 kcal/mol, respectively, calculated more simply by the Redhead method,[33] assuming first-order desorption kinetics and a preexponential factor of 10^{13} s^{-1}.

3.2. XPS. Figure 7 shows the C(1s) core-level photoelectron spectra corresponding to molecularly chemisorbed C_2D_2, as a function of C_2D_2 exposure on hex-Pt(100) at 100 K. The spectra are all described well by a single peak at 284.0 eV BE with a 2.0 eV full-width-at-half-maximum (fwhm). These results are consistent with a previous measurement of the C(1s) core level at 284.0 eV BE for molecular acetylene adsorbed on Pt(111).[34,35]

The C(1s) XPS spectra shown in Figure 8 were obtained after an exposure of 4 L C_2D_2 (to form a little more than a monolayer) on hex-Pt(100) at 100 K and stepwise annealing to higher temperatures. The C(1s) peak is 2.0 eV wide (fwhm) in each spectrum. Heating to 600 K caused the C(1s) peak to shift to

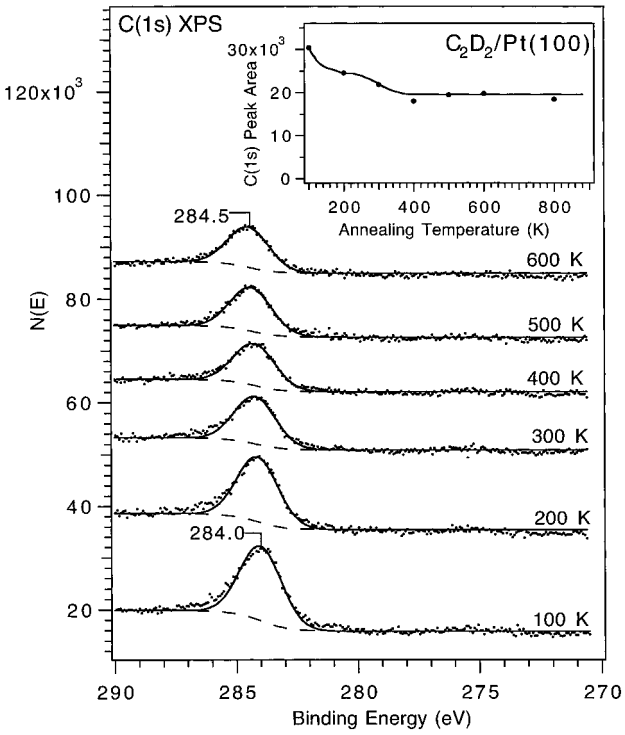

Figure 8. C(1s) spectra obtained as a function of annealing temperature following adsorption of a C_2D_2 monolayer on hex-Pt(100) at 100 K. The inset follows the associated C(1s) intensity changes with temperature.

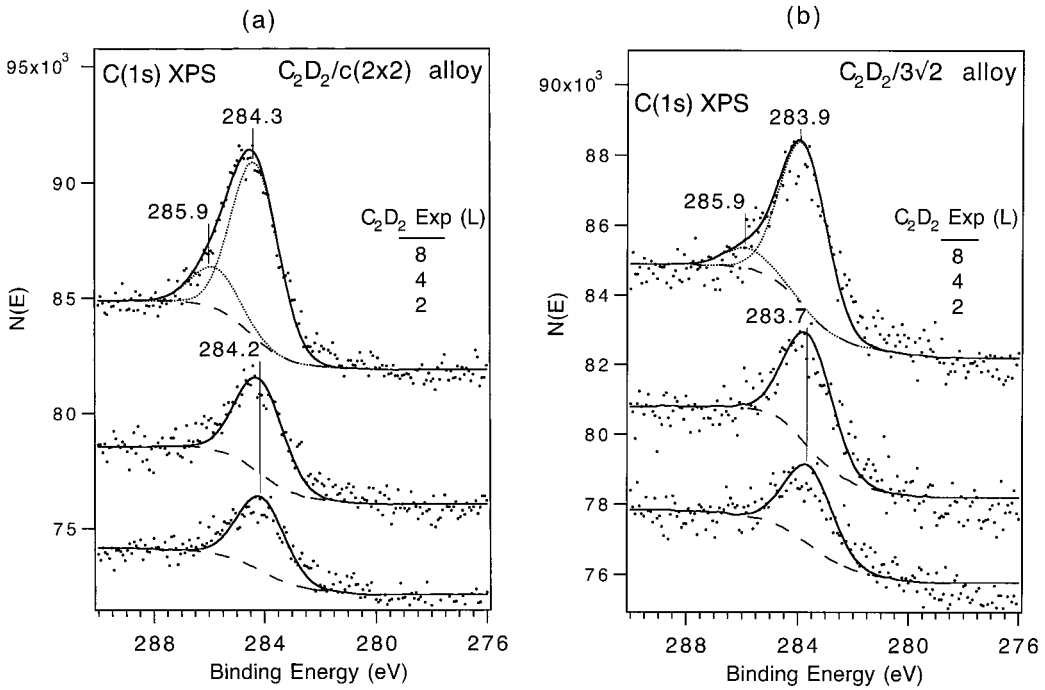

Figure 9. C(1s) spectra after acetylene exposures on the (a) c(2 × 2) alloy and (b) (3√2×√2)R45° alloy at 100 K.

0.5 eV higher BE, with the final value of 284.5 eV BE consistent with that for graphitic carbon at 284.3 eV BE on Pt(111).[34] The inset quantifies the corresponding C(1s) peak areas (the curve through the data also incorporates the observed TPD behavior). A decrease in the C(1s) intensity occurs after heating to 200 K because of the desorption of all physisorbed acetylene. An additional decrease of ~12% in the C(1s) intensity occurs after annealing the adlayer to 400 K. C_2D_4 desorption at 375 K is the main contribution to this decrease because of the very small amount of C_2D_2 desorption at 347 K (as will be seen later). The C(1s) intensity remained constant from 400 to 800 K, consistent with the absence of any significant desorption of hydrocarbons or diffusion of carbon into the bulk of the crystal.

C(1s) spectra for increasing C_2D_2 exposures on the c(2 × 2) and the 3√2 alloys at 100 K are shown in Figure 9a,b, respectively. The C(1s) peak for monolayer-C_2D_2 coverage is at 284.3 eV BE on the c(2 × 2) alloy and 283.9 eV BE on the 3√2 alloy. The peak width is 2.0 eV fwhm at low coverages on both surfaces, as on Pt(100), but the peak broadens to 2.6 eV at higher coverages. The C(1s) spectra after a dose of 8 L C_2D_2 in Figure 9 can be decomposed to give a new peak at 285.9 eV BE. We assign this peak to π-bonded acetylene molecules that are more loosely coordinated to the surface. Similar π-bonded acetylene species were found on Cs-modified Pd(110) surfaces.[36] In related studies, π-bonded ethylene species are formed on Cs/Pt(111) and K/Pt(111) surfaces.[37,38]

XPS was used in annealing studies on the 3√2 alloy in order to estimate the amount of benzene desorption. Figure 10 shows C(1s) spectra of a monolayer of adsorbed acetylene on the 3√2 alloy at 100 K and the adlayer formed after stepwise annealing. The inset quantifies the C(1s) intensity changes, with the solid curve drawn considering the observed TPD behavior. At 100 K, there are two peaks at 283.9 and 285.9 eV BE. The peak at 285.9 eV is eliminated by heating to 200 K, and the main C(1s) peak shifts to 0.9 eV lower BE. A new peak appears at 284.6 eV BE. A 20% decrease in the C(1s) intensity results from desorption of weakly adsorbed acetylene corresponding to the peaks in C_2D_2 TPD at 120 and 180 K. Heating to 300 K caused a large reduction in the C(1s) peak intensity corresponding to

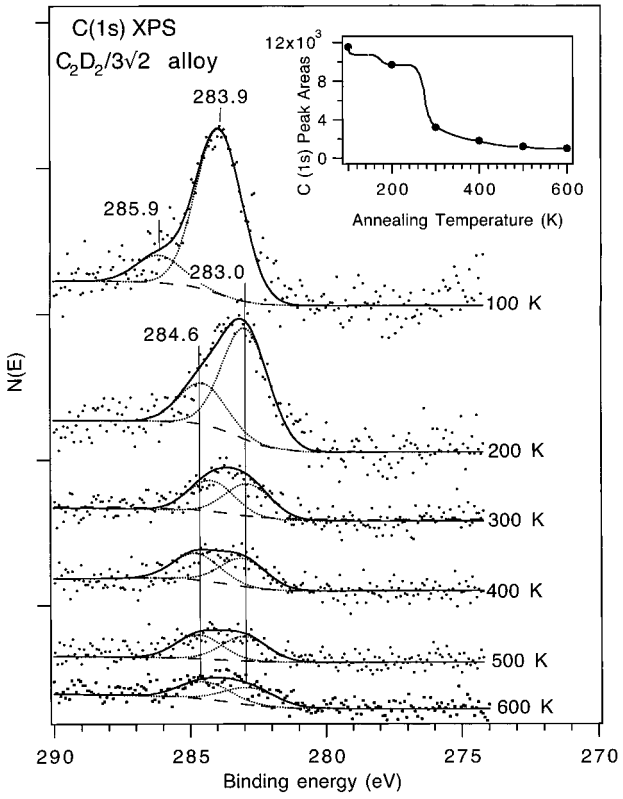

Figure 10. C(1s) spectra obtained as a function of annealing temperature following adsorption of a C_2D_2 monolayer on the (3√2×√2)-R45° alloy at 100 K. The inset shows the C(1s) intensity changes with annealing temperature.

molecular desorption of the 75% of the acetylene monolayer that is reversibly adsorbed. Two C(1s) peaks indicate the presence of more than one kind of surface species, (not from coadsorbed CO which would give rise to a peak at 286.7 eV[34]). Considering the TPD peak areas of C_2H_2 and C_6H_6, and also the decrease in C(1s) peak intensity by heating from 200 to 500 K, we conclude that ~15% of the adsorbed acetylene

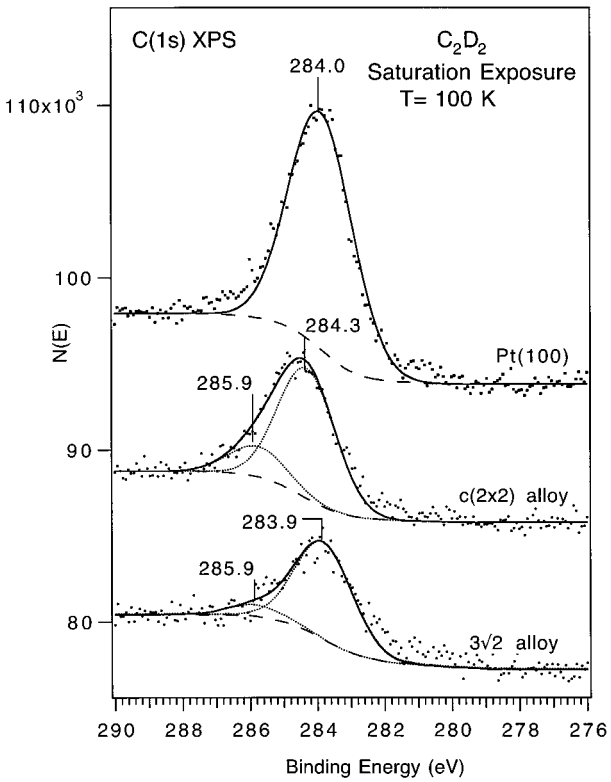

Figure 11. Comparison of the C(1s) spectra of an acetylene monolayer on several surfaces.

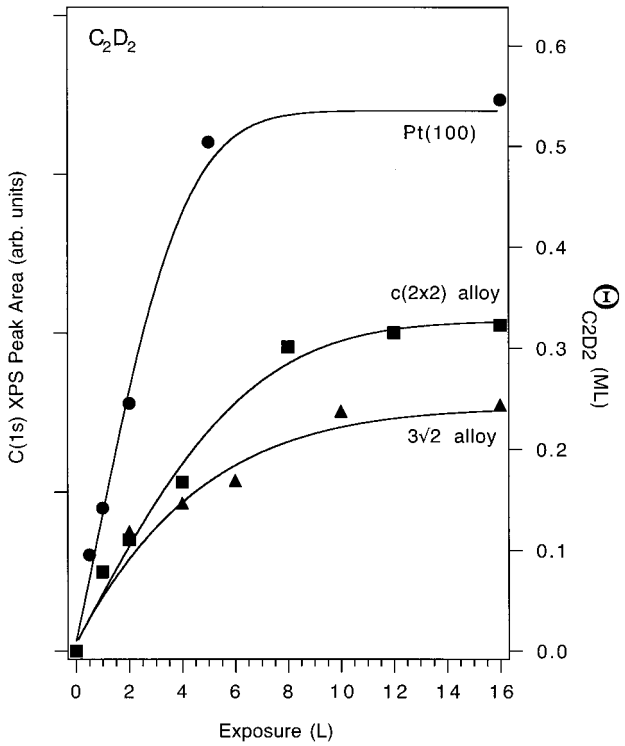

Figure 12. "Uptake curves" for the kinetics of C_2D_2 adsorption which were constructed from the C(1s) intensity in XPS on clean hex-Pt-(100) and the two alloyed surfaces. The C_2D_2 coverage indicated on the right-hand axis was estimated from the known saturation coverage of CO on the clean Pt(100) surface.[39]

monolayer undergoes cyclization to form benzene on the $3\sqrt{2}$ surface or $\theta_C^{rxn} = 0.04$ ML. The C(1s) intensity after annealing to 500 K indicates that a small amount (~5%) of decomposition occurs to form carbon on the surface. Adsorbed acetylene decomposed on the $3\sqrt{2}$ alloy to give two forms of carbon, i.e., graphitic (284.6 eV) and carbidic (283.0 eV) carbon, after heating to 600 K.[39]

The C(1s) spectra for monolayer coverages of acetylene on hex-Pt(100) and the two Sn/Pt alloy surfaces at 100 K are directly compared in Figure 11. We estimate that the coverage of acetylene in the chemisorbed monolayer on Pt(100) at 100 K is $\theta_{C_2D_2}^{sat} = 0.54$ ML. Our estimate is derived from a comparison with the C(1s) peak area from a monolayer of CO on Pt(100) at 100 K, where the CO coverage is known to be $\theta_{CO} = 0.75$ ML or 9.7×10^{14} molecules/cm^2.[39] This is consistent with a previous value of 0.5 ML at 328 K, which was derived from AES measurements.[4] The amount of acetylene adsorbed in the chemisorbed layer at 100 K is decreased due to the presence of alloyed Sn. The monolayer coverages of C_2D_2 on the c(2×2) and the $3\sqrt{2}$ Sn/Pt(100) alloys were determined to be 0.32 and 0.25 ML, respectively.

C(1s) data was also used to measure acetylene adsorption kinetics on the three surfaces at 100 K. Figure 12 shows "uptake curves," where the initial slope (at low exposures) is proportional to the initial sticking coefficient (S_0) of acetylene. The value of S_0 on both alloyed surfaces at 100 K is one-half of that on hex-Pt(100).

3.3. LEED. No extra spots in LEED were observed following acetylene adsorption on the c(2×2) or $3\sqrt{2}$ surfaces at 100 K. Either ordered adsorbate structures were not formed or ordered adlayer structures had the same size and orientation of their unit cells. Also, a number of annealing experiments were carried out up to 600 K following multilayer adsorption, and no new spots were observed at any time.

4. Discussion

On the hex-Pt(100) surface, ~90% of the chemisorbed acetylene monolayer decomposed to liberate D_2 and leave adsorbed carbon on the surface during heating in TPD. Molecular desorption of acetylene is minimal, but ~10% of chemisorbed acetylene undergoes hydrogenation and desorbs as ethylene at 375 K. C_2H_2 adsorbs on Pt(111) in a di-$\sigma + \mu_3$-η^2-π bonding fashion.[1-3] Presumably this occurs also on Pt(100) surfaces, but this determination must await vibrational studies.

Alloyed Sn at levels up to $\theta_{Sn} = 0.5-0.67$ ML on the Pt-(100) surface still allowed a large amount of acetylene to chemisorb. On the c(2×2) alloy, the acetylene monolayer coverage was $\theta_{C_2D_2}^{sat} = 0.32$ ML. Mainly desorption of molecular acetylene occurred, along with a small amount of D_2 desorption. The D_2 TPD peak areas and C(1s) intensity changes give a consistent estimate that 93% of the acetylene monolayer desorbed from the surface. The small amount of decomposition (~7%) may be due to defect sites, but most likely is not based on our experience. XPS and TPD spectra also show that a weakly bound species, which we assign to π-bonded acetylene, desorbs at 180 K on the c(2×2) alloy. Extensive molecular desorption of C_2D_2 (75%) occurs from the monolayer coverage of $\theta_{C_2D_2}^{sat} = 0.25$ ML on the $3\sqrt{2}$ alloy, along with benzene desorption.

Closely related studies have been reported for acetylene adsorption and reaction on Pt(111) and two Sn/Pt(111) surface alloys, a (2×2)Sn/Pt(111) alloy with $\theta_{Sn} = 0.25$ and a ($\sqrt{3} \times \sqrt{3}$)R30° Sn/Pt(111) alloy with $\theta_{Sn} = 0.33$ ML.[20] Alloying with Sn increased the molecular desorption of acetylene and inhibited decomposition. However, even on the $\sqrt{3}$ alloy, which has the highest Sn concentration, more than 35% of the chemisorbed acetylene monolayer decomposed to liberate H_2 and form surface carbon. The monolayer coverage decreased

about 20−25% upon alloying Sn into the Pt(111) surface.[20] This compares to a larger decrease of 40−60% on the Sn/Pt(100) alloys. The higher Sn concentration in the Sn/Pt(100) alloys isolates Pt atoms and thereby reduces pure Pt adsorption sites to a single Pt atom.

Given the very small changes detected in the Pt valence levels by UPS and core levels by XPS,[25,27] it is useful to attempt to understand the influence of Sn as due to "ensemble" effects. If such a simple interpretation were to explain the results, it would be useful for developing predictive capability (based simply on geometry) for other alloy surfaces. However, in doing so, it is also important to remember that changes in the Sn and Pt electronic structures ("ligand" effects) are still ultimately the important factors in the observed decrease in acetylene adsorption energy and increase in C−H dissociation activation energy barrier.

Looking at some specific ensembles that are available on the (2 × 2) Sn/Pt(111) alloy, 3-fold pure-Pt sites are present, but there are no two adjacent 3-fold pure-Pt sites. Only 2-fold bridge and atop sites are present on the $\sqrt{3}$ alloy, and all of the pure Pt 3-fold sites are eliminated. On the c(2 × 2) Sn/Pt(100) alloy, Pt atoms are isolated, surrounded only by nearest neighbor Sn atoms, and pure-Pt 2-fold bridge and 4-fold hollow sites are eliminated. (The $3\sqrt{2}$ alloy somehow incorporates additional surface Sn in a similar but unknown structure.) The strong suppression of decomposition of acetylene on both Sn/Pt(100) alloys can be attributed to an ensemble requirement of at least a pure Pt 2-fold bridge site to stabilize the transition state or reaction products of acetylene decomposition. Hence, acetylene decomposition at single Pt atoms on Pt−Sn alloys is a more highly activated process, compared to other available reaction channels, including acetylene desorption.

Benzene formation and desorption from cyclotrimerization reactions of acetylene on Pt−Sn alloys is a "structure-sensitive" reaction. Benzene desorption occurs from both of the Sn/Pt(111) alloys, with the highest amount of benzene (accounting for 10% of the acetylene monolayer) desorbing from the $\sqrt{3}$ surface.[20] Acetylene is strongly rehybridized on clean Pt(111), and benzene desorption from this reaction does not occur on Pt(111). Alloyed Sn weakens the Pt−C interaction, but this cannot be the only factor. If only a weaker interaction was required, then one would expect more benzene to desorb from the c(2 × 2) surface on Pt(100) with $\theta_{Sn} = 0.5$ ML than on the $\sqrt{3}$ Sn/Pt(111) surface with $\theta_{Sn} = 0.33$ ML. On the contrary, no benzene desorption was found on the c(2 × 2) alloy. However, it is well known that surface geometry plays a key role in benzene formation on Pd surfaces, and that is also apparently the case for Pt−Sn alloys. On the $3\sqrt{2}$ alloy with $\theta_{Sn} = 0.67$ ML, about 15% of the acetylene monolayer undergoes cyclotrimerization to form and desorb benzene. It is possible that benzene formation is a probe reaction for Pt ensembles that have hexagonal or (111)-like symmetry. This would imply that such facets or steps exist on the $3\sqrt{2}$ alloy. Consistent with that, CO chemisorption also reveals more Pt character on the $3\sqrt{2}$ alloy than on the c(2 × 2) alloy.[40] This could result from a higher Pt−Pt coordination number.

Figure 13 shows how the C_2D_2 monolayer coverage and initial sticking coefficient are affected by Sn addition to form surface alloys on the Pt(100) and Pt(111) surfaces. These curves provide a qualitative guide to the influence of alloyed Sn on acetylene chemisorption over a wide range of Sn concentrations, and more importantly, reveal whether specific site requirements exist. On Pt(111), the saturation coverage of acetylene has been reported to be 0.25 ML (3.8×10^{14} molecules/cm^2) at 100 K.[20,41] On

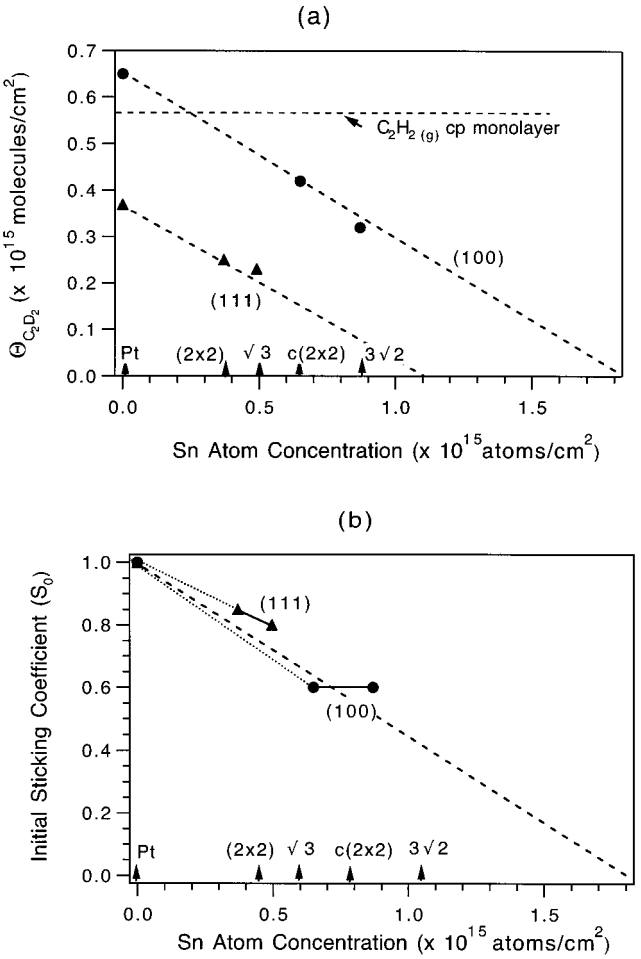

Figure 13. Influence of surface Sn concentration (atoms/cm^2) on Sn/Pt alloys at 100 K on (a) saturation-monolayer coverage $\theta_{C_2D_2}$ and (b) initial sticking coefficient S_0 of acetylene.

this basis, the saturation C_2H_2 coverage decreases to 0.17 ML on the (2 × 2) alloy and 0.16 ML on the $\sqrt{3}$ alloy at 100 K.[20] On Pt(100), the acetylene monolayer coverage has been reported to be 0.5 ML (6.5×10^{14} molecules/cm^2) at 100 K.[4,42] Using this reference, the monolayer coverage decreases to 0.32 ML on the c(2 × 2) alloy and 0.25 ML on the $3\sqrt{2}$ alloy at 100 K. The monolayer coverage is unexpectedly different on these two clean Pt surfaces, and so it is not surprising that there is some discrepancy about the monolayer coverage of acetylene on clean Pt(111).[20,35,41] This has been proposed to be either 0.25 ML[20,41] or 0.5 ML.[35] In Figure 13a we indicate the saturation monolayer coverage calculated from a closest packing (cp) model to give θ_{cp} with van der Waal's contacts using the C_2D_2 gas-phase structure. This coverage, $\theta_{cp} = 5.7 \times 10^{14}$ molecules/cm^2 (0.44 ML on Pt(100) and 0.37 ML on Pt(111)), sets a reasonable upper limit for the number of molecules in the chemisorbed layer. The coverage on Pt(100) has been reported to be slightly higher than θ_{cp}, but this can be explained by uncertainty in the experimental determination, or perhaps by the formation of either sp^2 or sp^3 hybridized species upon chemisorption which lead to slightly higher coverages. The changes in the chemisorbed monolayer coverage of C_2D_2 induced by Sn can be fit by a simple site-blocking model in which $\theta_{C_2D_2} = (1 - a\theta_{Sn})^b$, where $a = 1$ (the number of adsorption sites that are blocked by one modifier atom) and $b = 1$ (the number of adsorption sites required for adsorption) for both curves.

Values for the C_2D_2 initial sticking coefficient $S_0(C_2D_2)$ on the four Pt−Sn alloys at 100 K are compared in Figure 13b.

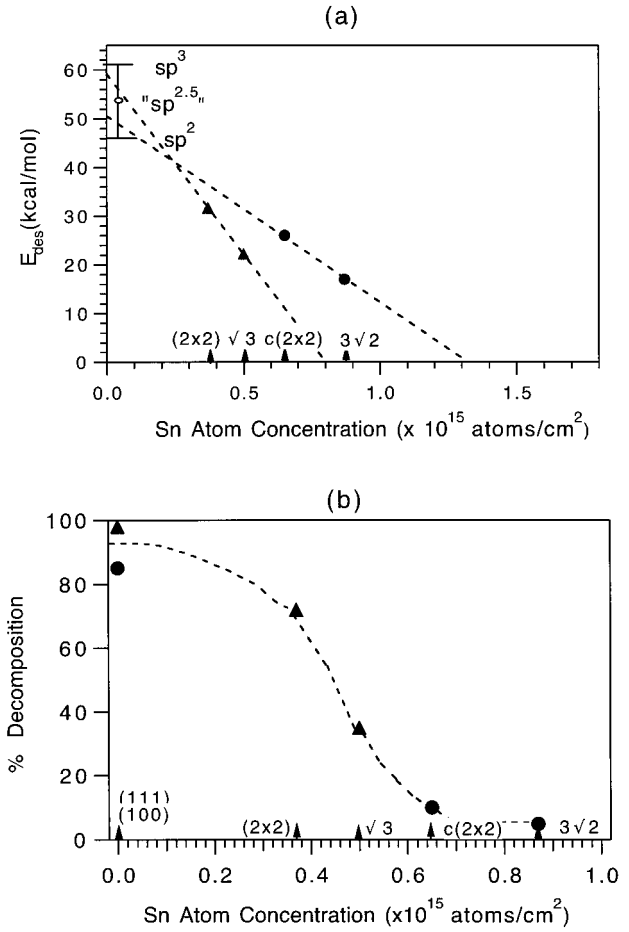

Figure 14. Influence of alloyed Sn on (a) the acetylene desorption activation energy E_d for the most strongly chemisorbed state and (b) the fractional amount of acetylene decomposition (normalized to the saturation monolayer coverage on each surface). Values given by the brackets in (a) for clean Pt(100) and Pt(111) surfaces are from predictions made in ref 45.

This behavior can be contrasted with that obtained for CO adsorption on these Pt−Sn surface alloys,[40] where a "modifier precursor" state had an important influence on the adsorption kinetics.[43,44] This factor allows for faster adsorption kinetics than would be expected for a linear or greater decrease in S_0 with increasing Sn concentration. A simple Langmuirian site-blocking equation for the dependence of S_0 is given by $S = S_0(1 - a\theta_{Sn})^b$, where $a = 0.8$ and $b = 1$ roughly accounts for the influence of alloyed Sn.

Figure 14a plots the desorption activation energy of acetylene on these surfaces, calculated using Redhead analysis. Because adsorption is not activated, these energies correspond to adsorption energies. The adsorption energy of acetylene on clean Pt(111) and Pt(100) surfaces can be estimated by extrapolating the adsorption energy curves to zero Sn concentration. We note that these values for acetylene adsorption on (111) and (100) Pt surfaces agree well with the "$sp^{2.5}$" adsorption energy of 54 kcal/mol predicted from sp^3(61 kcal/mol) and sp^2 (46 kcal/mol) C_2 species as estimated using the QVB theory by Koel and Carter[45] and a Pt−C covalent σ-bond strength of D(Pt−C) = 53 kcal/mol. Alloyed Sn weakens the chemisorption bond strength of acetylene by 45−65% on the Sn/Pt(100) alloys, and the acetylene desorption activation energy decreases in general with increasing surface Sn concentration. However, the C_2D_2 chemisorption bond strength on the c(2 × 2) Sn/Pt(100) alloy with $\theta_{Sn} = 0.5$ ML is apparently higher than that on the (2 × 2) Sn/Pt(111) alloy with $\theta_{Sn} = 0.33$ ML. This could arise from the different site symmetries presented on the two alloys.

The fraction of chemisorbed acetylene that decomposes to ultimately deposit carbon on the surface, i.e., the amount decomposed normalized to the monolayer coverage, is plotted in Figure 14b. The presence of ≥ 0.5 ML of Sn in the Pt(100) surface largely suppressed acetylene decomposition. Acetylene was reversibly adsorbed and desorbed on the Sn/Pt(100) alloys. Elimination of pure Pt 2-fold bridge and 4-fold hollow sites on the Sn/Pt(100) alloy surfaces indicates an ensemble requirement of at least a pure Pt 2-fold bridge site to stabilize the transition state for acetylene decomposition or the reaction products thus formed.

5. Conclusion

Alloying Sn to form the c(2 × 2) Sn/Pt(100) surface alloy, with $\theta_{Sn} = 0.5$, removes all pure Pt 4-fold hollow and pure Pt 2-fold bridge sites, leaving only isolated Pt surface atoms. There are many changes in acetylene adsorption and reaction caused by this modification, including a large suppression (more than 93%) of acetylene decomposition. The monolayer coverage of C_2D_2 decreases from 0.5 ML on Pt(100) to 0.32 ML on the c(2 × 2) alloy, and to 0.25 ML on another alloy, a $(3\sqrt{2}\times\sqrt{2})$-R45° structure with $\theta_{Sn} = 0.67$. Forming the c(2 × 2) alloy also reduced the initial sticking coefficient of acetylene on Pt(100) at 100 K by a factor of 2. Comparative studies of adsorption and reaction of acetylene on a c(2 × 2) Sn adlayer on Pt(100), with $\theta_{Sn} = 0.5$, demonstrate the importance of the position of Sn, in the adlayer or incorporated into the surface plane, in controlling site blocking. Acetylene chemisorption on these Sn/Pt alloyed surfaces is fairly structure insensitive, whereas acetylene decomposition is structure sensitive, and we propose that an ensemble of at least two contiguous Pt atoms is required for decomposition activity under these conditions. Cyclotrimerization of acetylene to benzene is also structure-sensitive and was observed only on the $(3\sqrt{2}\times\sqrt{2})$R45° Sn/Pt(100) alloy. This may be due to the presence of (111)-like steps or facets at this surface.

Acknowledgment. This work was supported by the U.S. Department of Energy, Office of Basic Energy Sciences, Chemical Sciences Division.

References and Notes

(1) Salmeron, M.; Somorjai, G. A. *J. Phys. Chem.* **1982**, *86*, 341.
(2) Megiris, C. E.; Berlowitz, P.; Butt, J. B.; Kung, H. H. *Surf. Sci.* **1985**, *159*, 184.
(3) Avery, N. R. *Langmuir* **1988**, *4*, 445.
(4) Fisher, T. E.; Kelemen, S. R.; Bonzel, H. P. *Surf. Sci.* **1977**, *64*, 157.
(5) Zhou, Y.; Davis, S. M. *Catal. Lett.* **1992**, *15*, 51.
(6) Cortright, R. D.; Dumesic, J. A. *J. Catal.* **1994**, *148*, 771.
(7) Paffett, M. T.; Gebhard, S. C.; Windham, R. G.; Koel, B. E. *Surf. Sci.* **1989**, *223*, 448.
(8) Xu, C.; Koel, B. E.; Paffett, M. T. *Langmuir* **1994**, *10*, 166.
(9) Tsai, Y. L.; Koel, B. E. *Surf. Sci.* **1997**, *385*, 37.
(10) Tysoe, W. T.; Nyberg, G. L.; Lambert, R. M. *J. Chem. Soc., Chem. Commu.* **1983**, 623.
(11) Patterson, C. H.; Lambert, R. M. *J. Am. Chem. Soc.* **1988**, *110*, 6871.
(12) Ormerod, R. M.; Lambert, R. M. *Catal. Lett.* **1990**, *6*, 121.
(13) Gellman, A. J. *J. Am. Chem. Soc.* **1991**, *113*, 4435.
(14) Avery, N. A. *J. Am. Chem. Soc.* **1985**, *107*, 6711.
(15) Lomas, J. R.; Baddeley, C. J.; Tikhov, M. S.; Lambert, R. M. *Langmuir* **1995**, *11*, 3048.
(16) Bertolini, J. C.; Massardier, J.; Dalmai-Imelik, G. *J. Chem. Soc., Faraday Trans.* **1978**, *I*, 1720.
(17) Yang, Q. Y.; Maynard, K. T.; Johnson, A. D.; Ceyer, S. T. *J. Chem. Phys.* **1995**, *102*, 7734.
(18) Gentle, T. M.; Muetterties, E. L. *J. Phys. Chem.* **1983**, *87*, 2469.

(19) Pierce, K. J.; Barteau, M. A. *J. Phys. Chem.* **1994**, *98*, 3882.
(20) Xu, C.; Peck, J. W.; Koel, B. E. *J. Am. Chem. Soc.* **1993**, *115*, 751.
(21) Ormerod, R. M.; Baddeley, C. J.; Lambert, R. M. *Surf. Sci*. **1991**, *259*, L709.
(22) Baddeley, C. J.; Ormerod, R. M.; Stephenson, A. W.; Lambert, R. M. *J. Phys. Chem.* **1995**, *99*, 5146.
(23) Baddeley, C. J.; Tikhov, M.; Hardacre, C.; Lomas, J. R.; Lambert, R. M. *J. Phys. Chem.* **1996**, *100*, 2189.
(24) Windham, R. G.; Paffett, M. T. *Surf. Sci.* **1989**, *208*, 34.
(25) Overbury, S. H.; Mullins, D. R.; Paffett, M. T.; Koel, B. E. *Surf. Sci.* **1991**, *254*, 45.
(26) Behm, R. J.; Hösler, W.; Ritter, E.; Binnig, G. *Phys. Rev. Lett.* **1986**, *56*, 228.
(27) Paffett, M. T.; Logan, A. D.; Simonson, R. J.; Koel, B. E. *Surf. Sci.* **1991**, *250*, 123.
(28) Li, Y.; Koel, B. E. *Surf. Sci.* **1995**, *330*, 193.
(29) Windham, R. G.; Bartram, M. E.; Koel, B. E. *J. Phys. Chem.* **1988**, *92*, 2862.
(30) Tsai, Y.-L. *Surface Science Studies of Thermal and Electron-Induced Reactions on Metal and Semiconductor Surfaces*, Ph.D. Thesis 1995, University of Southern California, p 210.
(31) Hoheisel, M.; Kuntze, J.; Speller, S.; Postnikov, A.; Heiland, W.; Spolveri, I.; Bardi, U. to be published.
(32) Norton, P. R.; Davies, J. A.; Creber, D. K.; Sitter, C. W.; Jackman, T. E. *Surf. Sci.* **1981**, *108*, 205.
(33) Redhead, P. A. *Vacuum* **1962**, *12*, 203.
(34) Freyer, N.; Pirug, G.; Bonzel, H. P. *Surf. Sci*. **1983**, *125*, 327.
(35) Freyer, N.; Pirug, G.; Bonzel, H. P. *Surf. Sci.* **1983**, *126*, 487.
(36) Takaoka, T.; Sekitani, T.; Aruga, T.; Nishijima, M. *Surf. Sci.* **1994**, *306*, 179.
(37) Cassuto, A.; Mane, M.; Hugenschmidt, M.; Dolle, P.; Jupille, J. *Surf. Sci*. **1990**, *237*, 63.
(38) Cassuto, A.; Mane, M.; Jupille, J.; Tourillon, G.; Parent, P. *J. Phys. Chem*. **1992**, *96*, 5987.
(39) Borden, G.; Pirug, G.; Bonzel, H. P. *Surf. Sci.* **1978**, *72*, 45.
(40) Panja, C.; Koel, B. E. *Isr. J. Chem.* **1998**, *38*, 365.
(41) Abon, M.; Billy, J.; Bertolini, J. C. *Surf. Sci*. **1986**, *171*, L387.
(42) Fischer, T. E.; Kelemen, S. R. *J. Vac. Sci. Technol*. **1977**, *15*, 607.
(43) Jiang, L. Q.; Koel, B. E.; Falconer, J. L. *Surf. Sci.* **1992**, *273*, 273.
(44) Xu, C.; Koel, B. E. *J. Chem. Phys.* **1994**, *100*, 664.
(45) Koel, B. E.; Carter, E. A. *Surf. Sci.* **1990**, *226*, 339.